

# JOURNAL OF THE AMERICAN CHEMICAL SOCIETY

Registered in U.S. Patent Office. © Copyright, 1978, by the American Chemical Society

VOLUME 100, NUMBER 1

JANUARY 4, 1978

## Qualitative Potential Energy Surfaces. 1. Theory

N. D. Epiotis\* and S. Shaik

Contribution from the Department of Chemistry, University of Washington,  
Seattle, Washington 98195. Received January 13, 1977

**Abstract:** The linear combination of fragment configurations approach is used in order to construct qualitative potential energy surfaces. The interaction of diabatic surfaces and the formation of reaction barriers and intermediates are discussed. The method is utilized to classify chemical reactions according to the polarity interrelationship between the lowest charge transfer ( $D^+A^-$ ) and no bond (DA) diabatic surfaces. The effect of polarity on barrier height, decay efficiency, and reaction selectivity is discussed. Experimental evidence is provided in support of the predictions.

### I. Introduction

In 1965, Woodward and Hoffmann suggested that a correlation exists between MO phase properties and certain reactivity trends.<sup>1</sup> Subsequently, Woodward and Hoffmann,<sup>2</sup> as well as Longuet-Higgins and Abrahamson,<sup>3</sup> showed that MO and state correlation diagrams can be used to achieve a satisfactory understanding of reaction mechanisms. These diagrams constitute a systematic attempt to construct qualitative potential energy (PE) surfaces. The major limitation of this approach is twofold: specifically, it fails to reveal barriers and intermediates in certain types of reactions. In addition, it cannot be applied directly to reactions which involve the making or breaking of a single bond. Finally, this method is restricted in application to "nonpolar" reactions and no attempts were made to investigate the "polar" extreme of the spectrum of chemical reactions.

In the early 1970s, one of the authors suggested that a correlation exists between the donor-acceptor matching of the reactants and various reactivity trends.<sup>4,5</sup> Two formalisms were proposed, the first using wave functions confined to the two reactants<sup>4</sup> and the second using totally delocalized wave functions.<sup>5</sup> This work constitutes the next step in the natural evolution of these theoretical ideas and delineates a qualitative theory which makes possible the construction of PE surfaces and, thus, the identification of barriers and intermediates.

### II. Theory

Consider a reaction between a donor molecule (or fragment) designated by D, and an acceptor molecule (or fragment) designated by A. The electronic states of the composite system D-A at a given intermolecular distance can be described in terms of a linear combination of fragment configurations (LCFC) method.<sup>6</sup> A complete knowledge of the eigenvalues and eigenvectors of the states of D-A for any geometrical arrangement leads to a satisfactory understanding of the chemical behavior of the system.

The first step in the analysis involves the choice of the basis set of zero-order configuration wave functions. For the purpose of illustrating the key theoretical principles, we shall consider the simple example of a basis set spanning the following zero-order configurations: (1) the no-bond configuration DA; (2) the locally excited configuration  $DA^*$ ; (3) the charge transfer configuration  $D^+A^-$ .

The three zero-order configurations are schematically represented in Figure 1a. The term configuration will be taken to mean a spin and symmetry adapted<sup>7</sup> wave function while the term zero-order configuration means the basic one-determinantal wave function describing the occupancy of the MOs of a fragment.

Our next task is to define the Hamiltonian operator, recalling that we shall be dealing with reactions which involve formation of one or more bonds at the transition state.

$$\hat{H} = \hat{H}_D + \hat{H}_A + \hat{P} \quad (1)$$

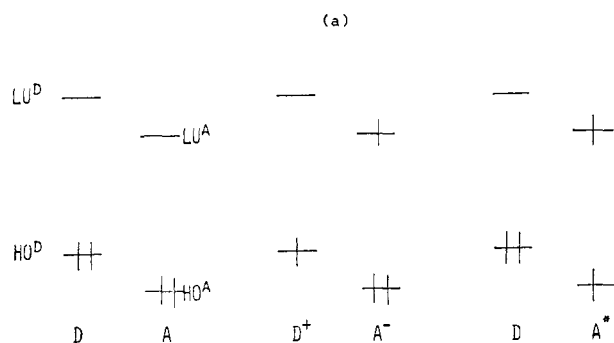
In eq 1,  $\hat{H}_D$  operates only on fragment D,  $\hat{H}_A$  operates only on fragment A, and  $\hat{P}$  operates along the forming bonds. Now, we can assume that the MOs of fragment D are orthogonal with respect to  $\hat{H}_D$  and the MOs of fragment A are orthogonal with respect to  $\hat{H}_A$ , whereas  $\hat{P}$  is an effective one-electron operator responsible for mixing the configurations. The equations which describe the energy dependence of each diagonal element of the energy matrix upon intermolecular distance, i.e., the equations of the diabatic surfaces, are approximated empirically below<sup>8</sup>

$$\epsilon(\text{DA}) = S(r) \quad (2)$$

$$\epsilon(\text{D}^+\text{A}^-) = I_D - A_A + C(r) + S'(r) \quad (3)$$

$$\epsilon(\text{DA}^*) = G_A(\text{HO}^A \rightarrow \text{LU}^A) + S'(r) \quad (4)$$

in terms of the ionization potential of the donor,  $I_D$ , the electron affinity of the acceptor,  $A_A$ , the  $\text{HO} \rightarrow \text{LU}$  transition energy of the acceptor,  $G_A$ , the Coulombic energy,  $C$ , and the steric



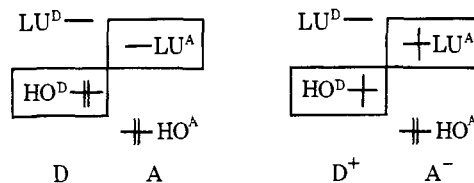
**Figure 1.** (a) The DA,  $D^+A^-$ , and  $DA^*$  zero-order basis set configurations. (b) Interaction matrix for the DA,  $D^+A^-$ , and  $DA^*$  basis set. D = donor, A = acceptor.

functions  $S$  and  $S'$ . A steric function describes two effects which obtain as the molecules combine to form a product: (a) The effect of steric repulsion which manifests itself as the two reactants approach each other. (b) The effect of bond readjustment necessary for transforming reactants to products. In this case, the energy required for stretching or compressing bonds, denoted by  $L$ , is a function of the MO occupancy of the two reactants in the zero-order basis set configuration. Thus,  $L$  is large in the case of the DA diabatic surface because each reactant has a maximum bonding occupancy, i.e., the bonding MOs of each reactant are all occupied and any geometrical change which will tend to deemphasize the bonding AO interactions will raise significantly the energy of the system. In the case of the  $D^+A^-$  and  $DA^*$  diabatic surfaces,  $L$  becomes smaller because both configurations involve an excitation of an electron from a bonding to an antibonding MO. As a result, a geometric deformation which will tend to deemphasize the bonding AO interactions will have a lesser effect on the energy of the  $D^+A^-$  and  $DA^*$  than on the energy of the DA diabatic surface.

A few observations on the shapes of the diabatic curves are now appropriate: (a) *A diabatic surface of the no-bond or local excitation type is repulsive.* The rise of the energy of such a diabatic surface as internuclear distance decreases is described by the appropriate steric function. (b) A diabatic surface of the charge transfer type has an attractive component ( $C$ ) and a repulsive component ( $S$ ). *Such a surface displays a minimum.* (c) The steric functions can be defined empirically or calculated in a way which can lead to quantitative estimates of reaction barriers. However, since we are interested in qualitative trends, we shall not define the various steric functions explicitly, but, rather, restrict ourselves to the qualitative drawing of the shapes of the diabatic surfaces.

Once we have discussed the diagonal elements of the energy matrix, we proceed to consider the interaction matrix elements which are evaluated with neglect of interfragmental MO overlap.<sup>9</sup> In such a case the matrix element between two configurations,  $\Psi_\rho$  and  $\Psi_\sigma$ , is reduced to a matrix element between the two MOs,  $\psi_\mu$  and  $\psi_{\mu'}$ , which differ in occupancy by one

**Scheme I.** Interacting Matrix Element between the Lowest Charge Transfer ( $D^+A^-$ ) and No-Bond (DA) Zero Order Configurations



electron in the two configurations.

$$P_{\rho\sigma} = \langle \Psi_\rho | \hat{P} | \Psi_\sigma \rangle = \langle \psi_\mu | \hat{P} | \psi_{\mu'} \rangle \quad (5)$$

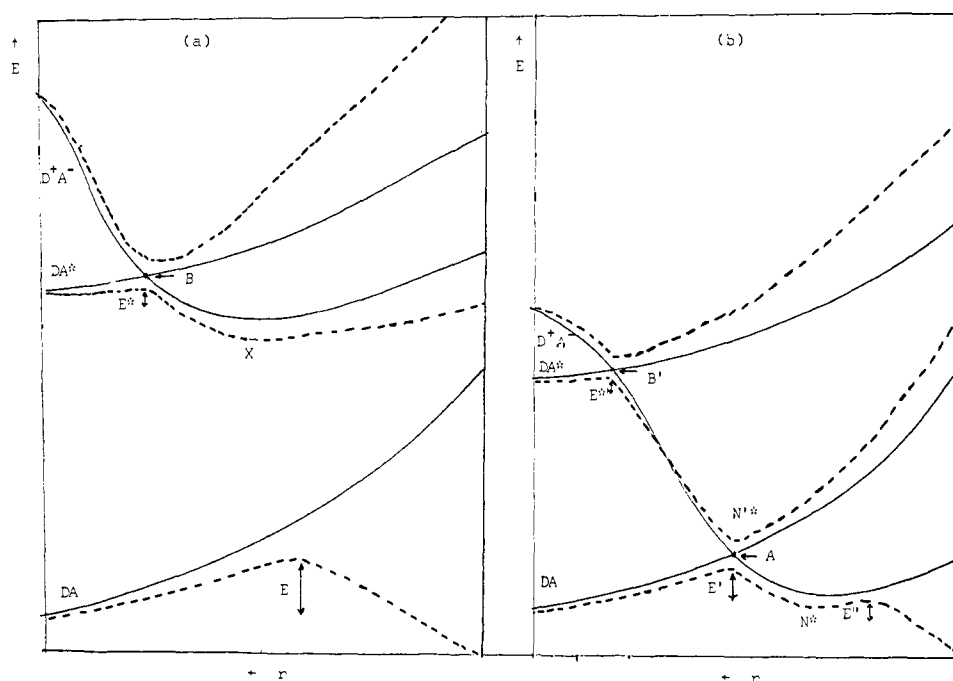
For example, consider the interaction matrix element of the DA and  $D^+A^-$  zero-order configurations shown in Scheme I. The two MOs which differ in occupancy by one electron in the two configurations are  $HO^D$  and  $LU^A$ . This matrix element can be approximated in terms of the corresponding overlap integral  $\langle HO^D | LU^A \rangle$ . Henceforth, one-electron interaction matrix elements between MOs will be set proportional to the corresponding MO overlap integral.<sup>10</sup> We shall use the symbol  $\mu-\mu'$  to designate the MO overlap integral  $S_{\mu\mu'}$ , dropping the necessary normalization constants for brevity. Using this convention, the interaction matrix for the problem at hand can be easily constructed. The results are given in Figure 1b. The form of the interaction matrix element, or the form of the corresponding MO overlap integral, is extremely important because it can be connected with important reaction aspects, such as stereoselectivity and regioselectivity.

Returning to our example, we assume a commonly occurring situation for which the  $HO^D-LU^A$  and  $HO^D-HO^A$  matrix elements are nonzero. Furthermore, we distinguish two different cases, namely, a situation where the DA and  $D^+A^-$  diabatic surfaces cross and another where they do not cross. A reaction which fulfills the first condition will be termed ionic, while a reaction which fulfills the second condition will be termed nonionic.

**A. Nonionic Reactions.** The diabatic and adiabatic PE surfaces for nonionic reactions are shown in Figure 2a. The adiabatic ground surface arises from the interaction of the no-bond (DA) and the charge transfer ( $D^+A^-$ ) diabatic surfaces. This interaction is of the  $HO^D-LU^A$  type (Figure 1b). As the intermolecular distance,  $r$ , decreases, the overlap between the two reactants increases and the interaction between the two diabatic surfaces increases, causing a bending of the ground adiabatic surface and resulting in the formation of barrier  $E$  in the direction of the final products.

The first excited surface results primarily from the interaction between the locally excited ( $DA^*$ ) and the charge transfer ( $D^+A^-$ ) diabatic surfaces ( $HO^D-HO^A$  type) and displays a barrier,  $E^*$ , at the intended crossing point B. Past the barrier, an excited intermediate  $X^{11}$  may be formed and decay across a large energy gap to the ground surface.

**B. Ionic Reactions.** The diabatic and adiabatic PE surfaces for the ionic reaction are shown in Figure 2b. The adiabatic ground surface arises from the interaction between the DA and the  $D^+A^-$  diabatic surfaces. This interaction is of the  $HO^D-LU^A$  type and increases as  $r$  decreases. In contrast with the previous case of nonionic reaction, a *ground* intermediate,  $N^*$ ,<sup>12</sup> will be accommodated in the energy well located about the minimum of the  $D^+A^-$  diabatic surface. The  $N^*$  intermediate can dissociate back to ground-state reactants by passage over barrier  $E'$  or collapse to product via passage over barrier  $E''$ . The  $E'$  barrier arises from the intended diabatic surface crossing between  $D^+A^-$  and DA (point A in Figure 2b) and the  $E''$  barrier arises from the gradually increasing interaction between the  $D^+A^-$  and the DA diabatic surfaces which causes bending of the adiabatic ground surface in the direction of the final ionic product. At long intermolecular

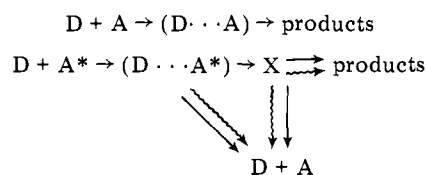


**Figure 2.** Diabatic (solid lines) and adiabatic (dashed lines) PE surfaces for (a) a nonionic reaction; (b) an ionic reaction, between a donor molecule D and an acceptor molecule A.

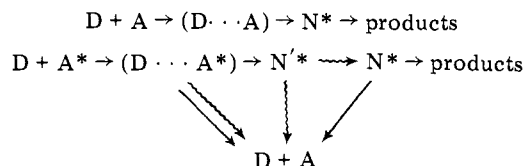
distances, the first excited surface arises primarily from the interaction of the  $D^+A^-$  and the  $DA^*$  diabatic surfaces ( $HO^D-HO^A$  type) and displays a barrier at the intended crossing point,  $B'$ . At shorter intermolecular distances, the shape of this surface is determined mainly by the interaction of the  $D^+A^-$  and the  $DA$  diabatic surface, and an excited intermediate  $N'^*$ <sup>13</sup> which is formed at the intended crossing point,  $A$ , can decay to the ground adiabatic surface.

The various conclusions can be conveyed with the aid of the following chemical equations, where  $D\cdots A$  and  $D\cdots A^*$  (in parentheses) are weak complexes which may be formed due to dominance of interfragment nucleus-electron attraction at long intermolecular distances.

#### A. Nonionic reactions



#### B. Ionic reactions



The above analysis projects a general pattern. In thermal reactions, we need be concerned only with barriers, while in photochemical reactions, we have to worry about barrier *plus* decay processes. While most chemists are familiar with the effect of barrier height upon reaction rate, the factors which control the efficiency of a decay process are many and, indeed, complicated. Various theoretical attempts toward understanding radiationless conversions have been made and quite a measure of success has been attained.<sup>14-16</sup> In order to develop an operationally workable scheme, we shall assume that the major factor which determines whether a given decay process will be fast is the energy gap  $\Delta Q$  between the two surfaces in-

volved. Specifically, we shall assume that as  $\Delta Q$  decreases the decay efficiency increases. Other factors, such as the slopes of the diabatic surfaces and the kinetic energy of the reaction partners,<sup>14</sup> are also important but will be neglected in the formulation of general predictive rules.

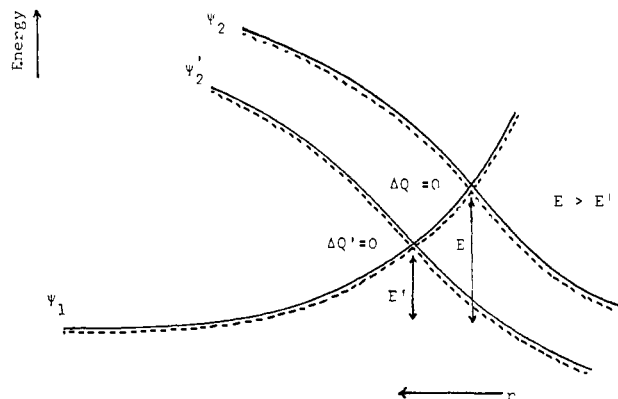
At this point, certain cautionary remarks are in order. Thus, Figures 2a and 2b display three intended diabatic surface crossings at  $A$ ,  $B$ , and  $B'$ . All these intended crossings become avoided owing to nonzero matrix elements. Further insight can be gained by realizing that actual crossings may be dependent upon the Hamiltonian employed in the evaluation of the interaction matrix elements. Accordingly, we can differentiate between two types of adiabatic surface crossings: (a) Real crossings which occur irrespective of whether the employed Hamiltonian contains only one-electron or both one-electron and two-electron parts. (b) Pseudocrossings, which occur when the employed Hamiltonian contains only one-electron parts.

By following the same line of reasoning, we can differentiate between two types of avoided adiabatic surface crossings: (a) First-degree avoided crossing due to the one-electron mixing of the diabatic surfaces. This situation arises when the employed Hamiltonian contains only one-electron parts. (b) Second-degree avoided crossings due to one-electron plus two-electron mixing of the diabatic surfaces. This situation arises when the employed Hamiltonian contains one-electron and two-electron parts.

As we have stated already, the LCFC method employs an effective one-electron Hamiltonian and, thus, in our discussions we shall always be concerned with first-degree avoided crossings and pseudocrossings. It is, then, apparent that, in dealing with pseudocrossings, the reader should remember that these are artifacts of the approximation involved in the LCFC method. He also should be aware of the fact that avoided crossings may be smaller or larger than actually depicted.

### III. The Interaction of Diabatic Surfaces

As we have already seen, in the process of constructing adiabatic PE surfaces, we encounter two general diabatic surface interrelationships. Namely, diabatic surfaces which cross and diabatic surfaces which do not do so. The interaction of such



**Figure 3.** The effect of translation of a diabatic surface  $\Psi_2$  to  $\Psi_2'$  on the energy barrier  $E$  and the energy gap  $\Delta Q$  for a case where the interaction matrix elements are zero.

diabatic surfaces at the crossing point and/or away from it has important chemical consequences, i.e., it controls barrier heights, stabilities of intermediates, and decay efficiencies. Accordingly, we should inquire as to how these reaction parameters vary as the relative energy of the interacting diabatic surfaces varies in a gradual manner. The diabatic surface energy variations crucial to this work are the following: (a) As reaction polarity increases, namely, as  $I_D - A_A$  decreases (eq 3), all charge transfer diabatic surfaces which involve transfer of electron(s) from the donor to the acceptor are translated downward in energy. Conversely, those which involve charge transfer in a reverse manner are translated upward in energy. (b) As the excitation energy of  $D$  and/or  $A$  decreases, the corresponding locally excited diabatic surfaces are translated downward in energy.

As an example, we consider the effect of polarity and excitation energy on barrier heights, decay efficiencies, and reaction selectivity in the case of two crossing diabatic surfaces,  $\Psi_1$  and  $\Psi_2$ . A downward translation of  $\Psi_2$  will lead to an earlier crossing, and will have the following consequences: (a) If the interaction matrix element is zero, the barrier  $E$  will decrease as the translation increases, while the energy gap between the resulting adiabatic surfaces  $\Delta Q$  will be zero throughout (Figure 3). (b) If the interaction matrix element is nonzero, reduced spatial overlap will diminish the absolute magnitude of the interaction matrix element. As a result, the barrier will decrease if the translation is much greater than the change of the interaction matrix element (Figure 4a) and vice versa (Figure 4b). On the other hand, the energy gap between the resulting adiabatic surfaces,  $\Delta Q$ , will shrink as translation increases. This will occur because the interaction matrix ele-

ment responsible for gap formation decreases in absolute magnitude owing to a progressive decrease of spatial overlap.

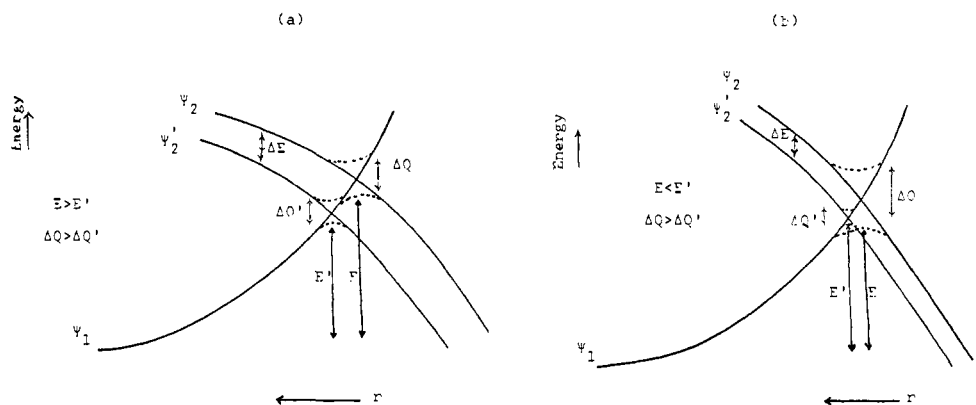
Next, we turn our attention to the problem of reaction selectivity. This corresponds to a case where the interaction matrix element, at the same intended crossing point, can assume two (or more) different values. Clearly, the corresponding interaction matrix elements will decrease as translation of  $\Psi_2$  increases. Consequently, the difference between the corresponding reaction barriers will shrink, i.e., there will be a decrease in reaction selectivity.

Similar arguments can be applied in a case of noncrossing diabatic surfaces. Once again, consider the interaction of two diabatic surfaces,  $\Psi_1$  and  $\Psi_2$ , away from an intended crossing point (Figure 5). As intermolecular distance decreases, the diabatic surfaces  $\Psi_1$  and  $\Psi_2$  begin to interact to an increasing extent, ultimately forming two adiabatic surfaces. As downward translation of  $\Psi_2$  increases, and assuming that  $\Psi_1$  and  $\Psi_2$  interact strongly, a lower and earlier barrier is formed on the  $\Phi_1$  adiabatic surface. This is an important point and the context in which this statement is made requires some illumination.

Consider the configurations  $\Psi_1$  and  $\Psi_2$  interacting at a large intermolecular distance,  $r'$ . In this case, their interaction is near zero because the corresponding matrix element is very small owing to negligible spatial overlap. At a moderate intermolecular distance,  $r''$ , interaction becomes possible and the energy of  $\Psi_1$  is lowered while that of  $\Psi_2$  is raised by the same amount, if overlap is neglected. The slope of the line  $PQ$  is an index of how fast the stabilization of  $\Psi_1$  due to its interaction with  $\Psi_2$  will tend to overtake the inherent energy increase of  $\Psi_1$ . In short, the stabilization of the  $\Psi_1$  configuration at an arbitrary intermolecular distance can be given the meaning of a slope. As stabilization increases owing to a downward translation of  $\Psi_2$ , the barrier  $E$  will tend to diminish and occur earlier on the reaction coordinate.

Let us now consider what happens when the interaction matrix element can take two different values. Once again, the difference in the stabilization of the  $\Psi_1$  configuration at an arbitrary intermolecular distance will have the meaning of a difference of two slopes. As a downward translation of  $\Psi_2$  occurs, the difference between the stabilization energies and, hence, the corresponding slopes will increase. Accordingly, when the diabatic surfaces do not cross, increasing reaction selectivity is expected to accompany an increase of reaction polarity.

We are now prepared to illustrate the application of the concepts delineated above to specific problems. For example, one expects the following trends as reaction polarity increases (as  $I_D - A_A$  decreases): (a) The barrier of a thermal nonionic



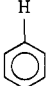

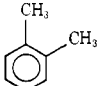
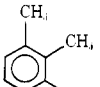
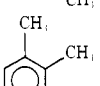
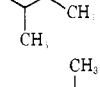
**Figure 4.** The effect of translation ( $\Delta E$ ) of a diabatic surface  $\Psi_2$  to  $\Psi_2'$  on the energy barrier  $E$  and the energy gap  $\Delta Q$ , in a case where the matrix elements are nonzero. (a) The change in the matrix element is smaller than the energy translation. (b) The change in the matrix element is larger than the energy translation.

**Table I.** Reactions of Dienophiles with Cyclopentadiene in Dioxane at 20 °C<sup>a</sup>

| Dienophile                             | 10 <sup>5</sup> k, L/mol s | Electron affinity, eV <sup>b</sup> |
|--|----------------------------|------------------------------------|
| (CN) <sub>2</sub> C=C(CN) <sub>2</sub> | ~43 000 000.00             | 3.89                               |
| (CN)HC=C(CN) <sub>2</sub>              | 483 000.00                 | ~2.10                              |
| H <sub>2</sub> C=C(CN) <sub>2</sub>    | 45 000.00                  | 1.54                               |
| (CN)HC=CH(CN)                          |                            |                                    |
| <i>cis</i> -                           | 91.00                      | 0.78 ± 0.1                         |
| <i>trans</i> -                         | 81.00                      | 0.78 ± 0.1                         |
| H <sub>2</sub> C=CH(CN)                | 1.04                       | 0.02                               |

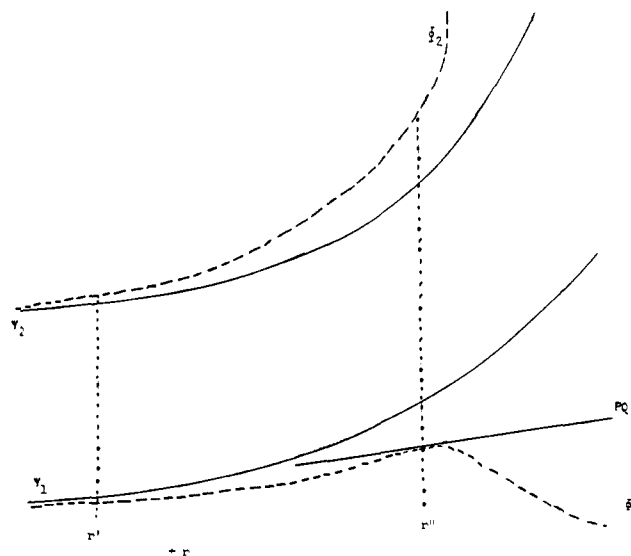
<sup>a</sup> See ref 17. <sup>b</sup> Electron affinity data are taken from K. N. Houk and L. L. Munchausen, *J. Am. Chem. Soc.*, **98**, 937 (1976).

**Table II.** Relative Rates of Bromination and Chlorination of Aromatic Hydrocarbons

| Aromatic substrate  | IP <sup>a</sup> | Relative rate of bromination in 85% HOAc <sup>b</sup> | Relative rate of chlorination in 85% HOAc <sup>b</sup> |
|---|-----------------|---|--|
|    | 9.25            | 1   | 1  |
|    | 8.90            | 650   | 340  |
|    | 8.60            | 5300  | 2030   |
|   | ~8.30           | 1 670 000   | 30 000 000   |
|  | ~8.00           | 11 000 000  |  |
|  | ~7.70           | 810 000 000   | 134 000 000  |

<sup>a</sup> IP values for benzene, toluene, and *o*-xylene from D. W. Turner, *Adv. Phys. Org. Chem.*, **4**, 30 (1960). The rest of the values are estimated. <sup>b</sup> See ref 18.

or ionic reaction, resulting from the interaction of DA and D<sup>+</sup>A<sup>-</sup> diabatic surfaces, will decrease. Exceptions will arise if the change of polarity is outweighed by a larger change of the corresponding interaction matrix element (HO<sup>D</sup>-LU<sup>A</sup>) operating in the opposite direction. The effect of polarity on reaction rates in Diels-Alder reactions of a donor with a series of acceptors has been studied experimentally<sup>17</sup> and typical data are displayed in Table I. As the acceptor strength of the dienophile increases, i.e., polarity increases, the reaction becomes faster. The same trend is observed in the case of ionic reactions, e.g., electrophilic aromatic substitutions<sup>18</sup> and ionic [2π + 2π] cycloadditions.<sup>19</sup> Typical data for electrophilic aromatic substitutions are displayed in Table II. (b) *The barrier of a photochemical reaction, arising from the interaction of DA\* and D<sup>+</sup>A<sup>-</sup> diabatic surfaces, will decrease.* Once again, exceptions will arise when a larger change of the interaction matrix element (HO<sup>D</sup>-LU<sup>A</sup>) counteracts a smaller change of polarity. Evidence for the effect of polarity increase on the relative efficiencies of photochemical reactions can be found in the photocycloaddition reactions of olefins with benzene.



**Figure 5.** Barrier formation via the interaction of two diabatic surfaces ( $\Psi_1$  and  $\Psi_2$ ) away from a crossing point. The stabilization of  $\Psi_1$  at  $r''$  or the slope of PQ are indices of the height of the barrier, and the looseness of the corresponding transition state. Solid lines indicate diabatic and dashed lines adiabatic surfaces ( $\Phi_1$  and  $\Phi_2$ ).

**Table III.** The Dependence of Product Distribution in the Electrophilic Substitution of Toluene on the Nature of the Electrophile

| Electrophile  | 2[para]/[ortho] <sup>a</sup> |
|---|------------------------------|
| <i>p</i> -CH <sub>3</sub> OC <sub>6</sub> H <sub>4</sub> CH <sub>2</sub> Cl/TiCl <sub>4</sub> | 5.00                         |
| <i>p</i> -CH <sub>3</sub> C <sub>6</sub> H <sub>4</sub> CH <sub>2</sub> Cl/TiCl <sub>4</sub>  | 4.17                         |
| <i>p</i> -HC <sub>6</sub> H <sub>4</sub> CH <sub>2</sub> Cl/TiCl <sub>4</sub>                 | 2.70                         |
| <i>p</i> -ClC <sub>6</sub> H <sub>4</sub> CH <sub>2</sub> Cl/TiCl <sub>4</sub>                | 2.70                         |
| <i>p</i> -NO <sub>2</sub> C <sub>6</sub> H <sub>4</sub> CH <sub>2</sub> Cl/TiCl <sub>4</sub>  | 1.15                         |
| <i>p</i> -CH <sub>3</sub> OC <sub>6</sub> H <sub>4</sub> SO <sub>2</sub> Cl/AlCl <sub>3</sub> | 33.30                        |
| <i>p</i> -CH <sub>3</sub> C <sub>6</sub> H <sub>4</sub> SO <sub>2</sub> Cl/AlCl <sub>3</sub>  | 12.50                        |
| <i>p</i> -HC <sub>6</sub> H <sub>4</sub> SO <sub>2</sub> Cl/AlCl <sub>3</sub>                 | 4.35                         |
| <i>p</i> -ClC <sub>6</sub> H <sub>4</sub> SO <sub>2</sub> Cl/AlCl <sub>3</sub>                | 2.94                         |
| <i>p</i> -NO <sub>2</sub> C <sub>6</sub> H <sub>4</sub> SO <sub>2</sub> Cl/AlCl <sub>3</sub>  | 1.61                         |

<sup>a</sup> See ref 18.

Thus, Bryce-Smith et al.<sup>20a</sup> reported that the quantum yield of the photocycloaddition of benzene and an olefin increases as the ionization potential of the olefin decreases. Typical data are shown below:

| Olefin                    | Ionization potential | $\Phi$ |
|---------------------------|----------------------|--------|
| <i>cis</i> -Cyclooctene   | 8.75                 | 0.09   |
| <i>trans</i> -Cyclooctene | 8.52                 | 0.37   |

Similarly, the photocycloaddition of benzene to acrylonitrile is enhanced (tenfold) in the presence of ZnCl<sub>2</sub>.<sup>20b</sup> The latter can coordinate with acrylonitrile and render it a better acceptor.<sup>21</sup>

Finally, we note an important difference between ionic and nonionic thermal reactions, namely, in the former case, selectivity will increase with polarity, whereas, in the latter case, the reverse trend is expected. Indeed, this is borne out by experimental evidence. Thus, the selectivity of a nonionic Diels-Alder reaction increases by Lewis acid catalysis<sup>22</sup> whereas that of an ionic electrophilic aromatic substitution reaction decreases as the electrophile becomes a better acceptor.<sup>18</sup> Typical data are displayed in Tables III and IV.

#### IV. Diabatic Surface Interrelationships. The Classification of Chemical Reactions

Having developed some key concepts on the basis of the dynamic LCFC method, we can now proceed to classify

**Table IV.** Regioisomer Ratio of Uncatalyzed and Lewis Acid Catalyzed Diels-Alder Reactions of Methylacrylate with Various Dienes<sup>a</sup>

| Diene                  | [Para]:[meta] |           |
|------------------------|---------------|-----------|
|                        | Uncatalyzed   | Catalyzed |
| 2-Phenyl-1,3-butadiene | 80:20         | 97:3      |
| 2-Chloro-1,3-butadiene | 87:13         | 98:2      |
| 2-Methyl-1,3-butadiene | 69:40         | 95:5      |
| 1-Methyl-1,3-butadiene | 90:10         | 98:2      |

<sup>a</sup> See ref 22.

chemical reactions according to the interrelationships of the diabatic surfaces which obtain in each case. One operationally useful classification is according to the interrelationship of the DA and D<sup>+</sup>A<sup>-</sup> diabatic surfaces. We distinguish the following types of reactions: (a) *nonionic reactions*, where the DA diabatic surface does not cross the D<sup>+</sup>A<sup>-</sup> diabatic surface; (b) *ionic reactions*, where DA crosses D<sup>+</sup>A<sup>-</sup> but the minimum of the D<sup>+</sup>A<sup>-</sup> diabatic surface lies above the minimum of the DA diabatic surface; (c) *superionic reactions*, where DA crosses D<sup>+</sup>A<sup>-</sup> and the minimum of the D<sup>+</sup>A<sup>-</sup> diabatic surface lies below the minimum of the DA diabatic surface.

Once a reaction has been classified in the manner suggested above, prediction of various reactivity aspects can be made. Clearly, what an experimentalist needs is some simple way of identifying the type of reaction at hand and, thus, anticipating its features. In proposing such an identification procedure, one must resort to approximations and generalizations. In this context, what follows constitutes only a model classification of chemical reactions which will undoubtedly be improved and refined further.

The proposed definitions are as follows:

(a) Nonionic reaction:  $I_D - A_A - C_m > 1.5$  eV

(b) Ionic reactions:  $I_D - A_A - C_m < 1.5$  eV

In the above inequalities,  $C_m$  is an average Coulombic attractive term for the range of intermolecular distances between 2.5 and 3.0 Å and the quantity  $I_D - A_A - C_m$  is assumed to be a satisfactory approximation of the energy of the D<sup>+</sup>A<sup>-</sup> diabatic surface near its minimum. Each definition is proposed on the basis of explicit test calculations and considerations of the experimental data. For example, the condition for an ionic reaction is that  $I_D - A_A - C_m$  should be less than 1.5 eV because the barrier of most thermal ionic reactions is of the order of magnitude of 1 eV.

It is obvious that the inequalities given above can be evaluated by reference to experimental or calculated ionization potentials and electron affinities. In addition, knowledge of the  $C_m$  term is demanded and this term can be easily calculated. However, in order to facilitate the procedure, the following  $C_m$  values are recommended:

(a) In reactions of simple molecules which are not highly conjugated,  $C_m$  will be taken equal to 5 eV.

(b) In reactions of highly conjugated molecules,  $C_m$  will be taken equal to 4 eV.

(c) In reactions where the positive hole is localized away from the framework where the negative excess is delocalized,  $C_m$  will be taken equal to 3 eV.

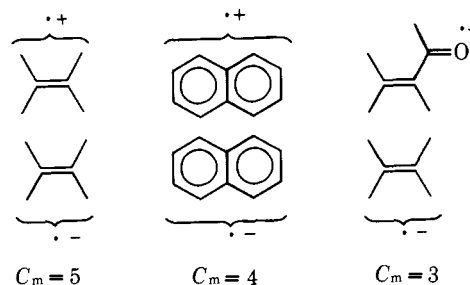
Typical examples of the three cases mentioned above are given in Chart I.

**Acknowledgment.** This work was supported by a NATO Grant (in collaboration with Professor F. Bernardi), and an A. P. Sloan Fellowship (1976-1978) to N.D.E.

## Appendix

The reduction of the rigorous LCFC theory to the qualitative scheme presented in this and subsequent papers is achieved in

Chart I



the following manner:



(a) The equations of the diabatic surfaces are written with respect to the total Hamiltonian. As an example, consider the prototype no-bond (DA) wave function  $1/\sqrt{4!}(1 - S^2) \cdot |\phi_A \phi_A \phi_B \phi_B\rangle$  shown schematically below:

$$\phi_{AD} \phi_{AB}$$

Assuming that  $\phi_A$  is centered on nucleus A and  $\phi_B$  is centered on nucleus B, and defining  $r$  as the distance of an electron in  $\phi_A$  from nucleus A,  $r'$  as the distance of an electron in  $\phi_B$  from nucleus B,  $r_{12}$  as the interelectronic distance,  $r_{AB}$  as the internuclear distance, and  $Z_A$  as the effective nuclear charge, the following equation results:

$$\begin{aligned} \langle DA | \hat{H} | DA \rangle = & \underbrace{\frac{2}{1-S^2} (\epsilon_A^0 + \epsilon_B^0) + \frac{1}{(1-S^2)^2} (J_{AA} + J_{BB})}_{Q} \\ & + \underbrace{\frac{2}{1-S^2} (V_A + V_B)}_R - \underbrace{\frac{4S}{(1-S^2)^2} (\langle AA | BA \rangle + \langle BB | BA \rangle)}_S \\ & + \underbrace{\frac{2}{(1-S^2)^2} [J_{AB}(2-S^2) - K_{AB}(1-3S^2)]}_T - \underbrace{\frac{4\beta S}{1-S^2} + V_{nn}}_U \end{aligned}$$

where

$$\epsilon_A^0 = \left\langle \phi_A \left| -\frac{1}{2}\nabla^2 - \frac{Z_A}{r} \right| \phi_A \right\rangle$$

$$J_{AA} = \left\langle \phi_A \phi_A \left| \frac{1}{r_{12}} \right| \phi_A \phi_A \right\rangle$$

$$S = \langle \phi_A | \phi_B \rangle$$

$$V_A = \left\langle \phi_A \left| \frac{-Z_B}{r'} \right| \phi_A \right\rangle$$

$$\langle AA | AB \rangle = \left\langle \phi_A \phi_A \left| \frac{1}{r_{12}} \right| \phi_A \phi_B \right\rangle$$

$$J_{AB} = \left\langle \phi_A \phi_A \left| \frac{1}{r_{12}} \right| \phi_B \phi_B \right\rangle$$

$$K_{AB} = \left\langle \phi_A \phi_B \left| \frac{1}{r_{12}} \right| \phi_A \phi_B \right\rangle$$

$$\beta = \left\langle \phi_A \left| -\frac{1}{2}\nabla^2 - \frac{Z_A}{r} - \frac{Z_B}{r'} \right| \phi_B \right\rangle$$

$$V_{nn} = \frac{Z_A Z_B}{r_{AB}}$$

The shape of the DA diabatic surface can be assessed qualitatively by examining the nature of the  $Q$ ,  $R$ ,  $S$ ,  $T$ ,  $U$ , and

Table V. The Effect of Exchange on the Shapes of Diabatic Surfaces<sup>a</sup>

| Item | Diabatic surface | LCFC-ZIDMOO                       |                                    | Rigorous LCFC                     |                                   |
|------|------------------|-----------------------------------|------------------------------------|-----------------------------------|-----------------------------------|
|      |                  | Aromatic <sup>b</sup> reaction    | Antiaromatic <sup>b</sup> reaction | Antiaromatic reaction             | Aromatic reaction                 |
| 1    |                  | R <sup>c</sup>                    | R <sup>c</sup>                     | R <sup>d</sup><br>(steep incline) | R <sup>d</sup><br>(small incline) |
| 2    |                  | AR                                | AR                                 | AR<br>(higher and looser minimum) | AR<br>(lower and tighter minimum) |
| 3    |                  | R <sup>c</sup>                    | R <sup>c</sup>                     | R <sup>d</sup>                    | R <sup>d</sup>                    |
|      |                  | Nonaromatic <sup>b</sup> reaction |                                    | Nonaromatic reaction              |                                   |
| 4    |                  |                                   | R <sup>e</sup>                     |                                   | AR                                |
| 5    |                  |                                   | AR                                 |                                   | AR                                |
| 6    |                  |                                   | R <sup>e</sup>                     |                                   | AR                                |

<sup>a</sup>R = repulsive, AR = attractive–repulsive. <sup>b</sup>In an aromatic reaction there is a symmetry congruence of HO<sup>D</sup>–LU<sup>A</sup> and HO<sup>A</sup>–LU<sup>A</sup>; in an antiaromatic reaction there is symmetry congruence of HO<sup>D</sup>–HO<sup>A</sup> and LU<sup>D</sup>–LU<sup>A</sup>; in a nonaromatic reaction there are no symmetry constraints. <sup>c</sup>Exaggerated minimum at long interfragment distance may exist. <sup>d</sup>Shallow minimum at long interfragment distance may exist. <sup>e</sup>Rigorous LCFC minimum may be reduced drastically and shifted to long intermolecular distance.

$V_{nn}$  terms. The variation of  $Q$  is small compared to all the other terms. Hence,  $Q$  can be regarded as invariant.  $R$  and  $-S$  are attractive terms, the former reflecting interfragment nucleus–electron attraction.  $T$  and  $-U$  are repulsive terms, the former reflecting Coulomb repulsion corrected for exchange correlation and the latter overlap repulsion. Finally,  $V_{nn}$  is a strong repulsive term from intermediate to short interfragment distances. The  $R$  plus  $-S$  contribution tends to cancel the  $T$  plus  $-U$  one and  $V_{nn}$  becomes responsible for a repulsive DA surface. Of course, other partitions are possible leading to the same result which has been tested by substituting representative quantities.

A simplification can be accomplished by neglecting differential interfragment overlap (zero interfragment differential MO overlap (ZIDMOO) approximation).

$$\langle DA | \hat{H} | DA \rangle = \underbrace{2(\epsilon_A^0 + \epsilon_B^0) + J_{AA} + J_{BB}}_{Q'} + \underbrace{2(V_A + V_B)}_{R'} + \underbrace{4J_{AB} + V_{nn}}_{S'}$$

$Q'$  is invariant to interfragment distance while  $R'$  is an attractive and  $S'$  a repulsive term. For the range of interfragment distances which are crucial to our discussions, the curve remains repulsive, albeit much less steep, owing to the strong influence of  $V_{nn}$  (however, vide infra). Of course, recognition of the fact that the two reactants do not combine in a frozen geometry and that an energetic price has to be paid for bond

and bond angle readjustments reinforces this conclusion.

By following a similar procedure, we can write the rigorous equations of  $D^+A^-$  and  $DA^*$  for the example of Figures 1 and 2. Qualitative considerations and substitution of representative values lead to the conclusion that the  $DA^*$  curve is repulsive while  $D^+A^-$  has a minimum at somewhat long interfragment distance. Application of the ZIDMOO approximation does not alter these qualitative conclusions, although the steepness of  $DA^*$  and the position of the  $D^+A^-$  minimum do change.

(b) The off-diagonal elements are written with respect to the total Hamiltonian. As an example, consider the matrix element  $\langle DA | \hat{H} | D^+A^- \rangle$ .

$$\begin{array}{cc} \phi_A \begin{array}{c} + \\ | \\ + \end{array} \phi_B & \phi_A \begin{array}{c} - \\ | \\ \# \end{array} \phi_B \\ D \quad A & D^+ \quad A^- \end{array}$$

$$\langle DA | \hat{H} | D^+A^- \rangle = \left( \frac{2}{1+S} \right)^{1/2} [\beta + (\epsilon_A^0 + V_A)S + \langle AA | AB \rangle]$$

Using well-known approximations (e.g.,  $\beta = kS$ , where  $k$  is an energy constant, etc.) an equation of the form shown below can be justified:

$$\langle DA | \hat{H} | D^+A^- \rangle \approx NS$$

Application of the ZIDMOO approximation simplifies the original equation as follows:

$$\langle DA | \hat{H} | D^+A^- \rangle = (2)^{1/2} \beta = k'S \quad (k' \text{ is an energy constant})$$

Once again, we find that qualitatively the interaction matrix element is a function of overlap although the preceding energy factor,  $k'$ , is different from  $N$ .

In short, the rigorous or ZIDMOO-LCFC method provides the basis for justifying the shapes of the diabatic PE surfaces which are crucial for an understanding of reactivity trends and the ZIDMOO-LCFC method provides a convenient short-cut in estimating interaction matrix elements. Some limitations of the ZIDMOO approximation are only quantitatively significant and do not affect qualitative predictions. Some problems are discussed below.

(a) At the level of the LCFC-ZIDMOO approximation, avoided crossings may become pseudocrossings. These cases are rather infrequent since most crossing diabatic surfaces arise from configurations which differ in the occupancy of a single spin MO and their interaction can be adequately described by the LCFC-ZIDMOO method. An example of a reaction where ground and diexcited diabatic surfaces intersect is the  $2\pi_S + 2\pi_S$  cycloaddition where the pseudocrossing becomes avoided when using the rigorous LCFC.

(b) The LCFC-ZIDMOO method may introduce unreasonably deep energy wells at long intermolecular distances in all diabatic surfaces where both components are closed shell or one open and the other closed shell. This can arise because interfragment nucleus-electron attraction may dominate nucleus-nucleus and electron-electron repulsion at such distances. Inclusion of exchange terms brings into fore overlap repulsion which can counteract this effect. The correct result is that weak molecular complexes may or may not be formed depending on the case at hand. Cognizant of this limitation of the LCFC-ZIDMOO approach, we have omitted weak complex minima in drawing certain diabatic surfaces but noted their possible existence in the chemical equations (in parentheses). The important thing is that these weak complexes are known from experimental studies to arise at long intermolecular distances much before the barrier peaks crucial to our arguments.

(c) The LCFC-ZIDMOO method may produce an incorrect shape for a diabatic surface of the no-bond or local excitation type where both components are open shell. In such a case, a loose and shallow minimum or no minimum at all, rather than the tight and deep minimum predicted by the rigorous LCFC method (assuming that at least one singly occupied AO of one fragment has symmetry congruent with at least one singly occupied AO of the second fragment), may be produced. For simplicity, we shall draw diabatic surfaces of this type as repulsive assuming that CI correction ultimately leads to the correct shape of the corresponding adiabatic surface. We find this to be generally true for most chemical problems of interest. This limitation does not affect qualitative arguments and an example will be given below.

(d) The LCFC-ZIDMOO method may produce similar shapes to those produced by the rigorous LCFC method with differences in the exact slopes or positioning of minima.

The results of a comparative study are summarized in Table V. These are restricted to three important types of diabatic surfaces which play a pivotal role in all reactions. Items 4 and 6 illustrate major modifications which, however, do not affect any of the qualitative conclusions. For example, the LCFC-

ZIDMOO method predicts that covalent bond strength depends primarily on the  $DA-D^+A^-$  interaction, a  $HO^D-HO^A$  interaction. On the other hand, the rigorous LCFC method predicts that the same quantity depends primarily on the exchange stabilization of the DA diabatic surface which, in turn, depends also on  $HO^D-HO^A$  interaction. Of course, part of covalent bonding is also due to  $DA-D^+A^-$  interaction according to the latter method. However, even in a quantitative sense, the problem can be treated at the LCFC-ZIDMOO level by appropriate parametrization of the  $HO^D-HO^A$  matrix element, i.e., the ZIDMOO approximation "turns off" the exchange stabilization of the DA configuration but this can be counteracted by appropriate parametrization of  $\beta$ .

## References and Notes

- (1) (a) R. B. Woodward and R. Hoffmann, *J. Am. Chem. Soc.*, **87**, 395 (1965); (b) R. Hoffmann and R. B. Woodward, *ibid.*, **87**, 2046 (1965); (c) R. B. Woodward and R. Hoffmann, *ibid.*, **87**, 2511 (1965).
- (2) R. B. Woodward and R. Hoffmann, "The Conservation of Orbital Symmetry", Verlag Chemie, Weinheim/Bergstr., Germany, 1970.
- (3) H. C. Longuet-Higgins and E. Abrahamson, *J. Am. Chem. Soc.*, **87**, 2045 (1965).
- (4) (a) N. D. Epiotis, *J. Am. Chem. Soc.*, **94**, 1924 (1972); (b) *ibid.*, **94**, 1935 (1972); (c) *ibid.*, **94**, 1941 (1972); (d) *ibid.*, **94**, 1946 (1972); (e) *Angew. Chem., Int. Ed. Engl.*, **13**, 751 (1974).
- (5) (a) N. D. Epiotis, *J. Am. Chem. Soc.*, **95**, 1191 (1973); (b) *ibid.*, **95**, 1200 (1973); (c) *ibid.*, **95**, 1206 (1973); (d) *ibid.*, **95**, 1214 (1973).
- (6) For previous applications of the LCFC theory to chemical problems, see (a) R. S. Mulliken and W. B. Person, "Molecular Complexes", Wiley-Interscience, New York, N.Y., 1969; (b) J. N. Murrell, "The Theory of the Electronic Spectra of Organic Molecules", Wiley, New York, N.Y., 1963; (c) S. P. McGlynn, L. G. Vanquickenborne, M. Kinoshita, and D. G. Caroll, "Introduction to Applied Quantum Chemistry", Holt, Rinehart and Winston, New York, N.Y., 1972.
- (7) For a discussion of symmetry and spin adaptation of determinantal wave functions, see ref 6c, Chapter 7.
- (8) This is a simplified version of a rigorous formalism where the elements of the energy matrix are evaluated with respect to a complete Hamiltonian and interfragment differential MO overlap is neglected. See Appendix.
- (9) Rules for evaluation of matrix elements between Slater determinants are described, inter alia, in (a) ref 6c; (b) W. G. Richards and J. A. Horsley, "Ab Initio Molecular Orbital calculations for Chemists", Clarendon Press, Oxford, 1970.
- (10) H. C. Longuet-Higgins and M. De V. Roberts, *Proc. R. Soc. London, Ser. A*, **224**, 336 (1954).
- (11) The symbol X denotes an intermediate which is described by a wave function with major charge transfer and local excitation and minor no-bond contributions.
- (12) The symbol N\* denotes an intermediate which is described by a wave function with major charge transfer and minor no-bond contribution.
- (13) The symbol N'\* denotes an intermediate which is described by a wave function which involves the "antibonding" combination of the DA and  $D^+A^-$  configurations.
- (14) (a) L. Landau, *Phys. Z. Sowjetunion*, **2**, 46 (1932); (b) C. Zener, *Proc. R. Soc. London, Ser. A*, **137**, 696 (1932).
- (15) (a) G. W. Robinson and R. P. Frosch, *J. Chem. Phys.*, **37**, 1962 (1962); (b) *ibid.*, **38**, 1187 (1963).
- (16) J. Jortner, *Pure Appl. Chem.*, **27**, 389 (1971).
- (17) R. Huisgen, R. Grashey, and J. Sauer in "The Chemistry of Alkenes", S. Patai, Ed., Interscience, New York, N.Y., 1964.
- (18) G. A. Olah, *Acc. Chem. Res.*, **4**, 240 (1971).
- (19) H. K. Hall, Jr., and P. Ykman, *J. Am. Chem. Soc.*, **97**, 800 (1975).
- (20) (a) D. Bryce-Smith, A. Gilbert, and B. Orger, *J. Chem. Soc., Chem. Commun.*, 334 (1974); (b) M. Ohasi, *Tetrahedron Lett.*, 3395 (1973).
- (21) This trend reverses toward the limit of highly polar nonionic photoreactions where the low energy of the  $D^+A^-$  minimum may become responsible for efficient decay of the excited intermediate X to ground state reactants (energy wasting photoreaction). For an analysis of this problem, see R. L. Yates, N. D. Epiotis, and S. Shaik, *J. Am. Chem. Soc.*, submitted for publication.
- (22) T. Inukai and T. Kojima, *J. Org. Chem.*, **32**, 869, 872 (1967); **36**, 924 (1971).
- (23) For example, see H. Umeyama and K. Morokuma, *J. Am. Chem. Soc.*, **98**, 7208 (1976), and previous papers.